Optical aggregation of metal nanoparticles in a microfluidic channel for surface-enhanced Raman scattering analysis

Lianming Tong,[a] Maurizio Righini,[b] Maria Ujue Gonzalez,[b] Romain Quidant[bc] and Mikael Käll[*a]

Aggregated metal nanoparticles exhibit enhanced electromagnetic fields that enable highly sensitive vibrational spectroscopy analysis based on surface-enhanced Raman scattering (SERS). We demonstrate SERS detection of organic analytes adsorbed to *optically aggregated* silver nanoparticles in a microfluidic device. The combination of optical tweezers and microfluidics technologies paves the way for novel lab-on-a-chip based plasmonic chemo/bio sensors and overcomes two important drawbacks of standard SERS sensing schemes; *i.e.* the renewal of nanofabricated metallic substrates and the difficulty of avoiding uncontrolled aggregation in metal colloids.

SERS is a powerful method for amplifying molecular Raman scattering cross-sections based on adsorption to metal nanostructures.[1] Typical enhancement factors range from 10^6 to 10^9, reaching the $\sim 10^{10}$ "single molecule level" in special cases.[2] SERS therefore has great potential in analytical chemistry and bio/chemo sensor development, in particular when applied to vibrational "fingerprint" spectra of organic molecules.[3,4] The SERS phenomenon originates in electromagnetic field-enhancement effects associated to density oscillations of the metal charge carriers, so-called localized surface plasmon resonances (LSPR's).[1] Silver and gold are the most suitable enhancing metals, due to their favourable plasmonic response in the visible wavelength range, but there are many degrees-of-freedom available in the actual design of a SERS substrate.[5] A multitude of Ag and Au SERS substrates has therefore been described in the literature.[6–9] Particularly large field-enhancement is achieved in systems of nearly touching particles, such as aggregated or close-packed colloids. However, from an application point of view, both surface supported nanostructures and colloidal solutions suffer drawbacks, *i.e.* the difficulty of cleaning the nanostructures for re-use and the difficulty of avoiding uncontrolled aggregation of colloids, respectively. Microfluidic-SERS has solved the former problem to a great extent.[10–12] However, most studies have relied on salt/analyte-driven aggregation of colloids, which is in general notoriously difficult to control.

In this communication, we report on SERS measurements of Ag colloids in a microfluidic circuit operated as a lab-on-a-chip device, where aggregation is achieved through optical forces generated by laser tweezers integrated into the Raman spectroscopy set-up.[13,14]

[a]Department of Applied Physics, Chalmers University of Technology, 41296 Göteborg, Sweden. E-mail: kall@chalmers.se
[b]ICFO - Institut de Ciències Fotòniques, Parc Mediterrani de la Tecnologia, 08860 Castelldefels(Barcelona), Spain
[c]ICREA - Institució Catalana de Recerca i Estudis Avançats, 08010 Barcelona, Spain

Laser tweezers are capable of trapping metal nanoparticles through field gradient forces directed towards the beam-waist of a tightly focused laser beam, where additional scattering and absorption forces tend to push the particles along the optical axis. In addition to these single particle forces, the laser field generates attractive inter-particle optical forces that result in colloidal aggregation. The application of the laser tweezers to a stream of metal colloids thus results in an accumulation and subsequent aggregation of nanoparticles at the laser tweezers focus. If the latter is positioned at the bottom of a microfluidic channel, the net result is a minuscule, but highly SERS active, surface supported particle aggregate. Moreover, the aggregate can in principle be controlled by applying appropriate laser tweezing power and irradiation time. We believe that this approach towards achieving controlled aggregation of plasmonic particles in microfluidic channels has great potential for the development of future lab-on-a-chip SERS sensors.

Fig. 1 shows a schematic picture of the experimental setup. Optical aggregation was achieved using a home-built laser tweezers setup integrated with a Renishaw 2000 Raman spectroscopy system. Raman excitation is achieved using the 514.5 nm output of an Ar$^+$ ion laser (Spectra Physics 2060), which also pumps the near-infrared (NIR) Ti:sapphire laser (Spectra Physics 3900S) used for laser tweezing. The NIR laser is tuned to 830 nm and delivers $\sim$90 mW at the sample, while the Raman excitation power is $\sim$3.5 mW. The two laser beams are coupled into a Leica DMLM microscope and focused on the sample through the same $100 \times$ objective lens (N.A. = 0.9). An oil immersion condenser (Nikon, N.A. = 1.2–1.4) is used for dark field (DF) imaging.

Ag colloids, with an average particle diameter of $\sim$40 nm and a concentration of $\sim$0.5 nM, were prepared according to the standard Lee and Meisel protocol.[15] Thiophenol (TP) and 2-naphthalenethiol (2-NT) were used as SERS analytes at a concentration of $\sim$50 μM.
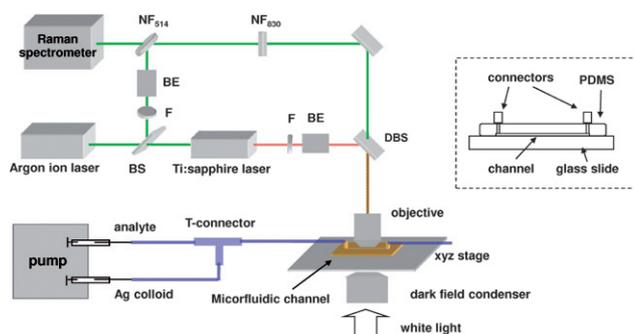

Fig. 1 Schematic of the experimental setup. Right inset: schematic of the microfluidic channel. Abbreviations: F for filter, BE for beam expander, DBS for dichroic beam splitter, and NF for notch filter.

The microfluidic channels were fabricated by photolithography in polydimethylsiloxane (PDMS) and attached on a clean glass slide. The right inset in Fig. 1 shows a schematic of a microfluidic sample. The height and width of the channel are 25 μm and 500 μm, respectively, and the length is ~4 cm. The thickness of the PDMS layer is ~130 μm and that of the bottom glass slide is 150 μm. A T-connector is used at the inlet side, so that the Ag colloid and analytes are injected separately and mix at the T-cross, where incubation begins. In a second configuration, with a Y-shaped microfluidic channel, the parameters are the same except that the widths of both input channels are 300 μm. All the tubings are made of Teflon and have 0.3 mm inner diameter. A pump (Harvard PHD 2000 Infusion) is used to drive the syringes.

Fig. 2(a) shows a 20× DF image of a microfluidic channel captured with the pump turned off. Isolated diffusing Ag nanoparticles are visible as tiny whitish speckles. Fig. 2(b) shows images captured with a 100× objective during a trapping experiment with the 830 nm laser. The flow rate is here set to 1.0 μl/min, which corresponds to an approximate particle flow speed of ~1.3 mm/s. This is too fast for the camera to be able to capture single flowing particles, which instead gives rise to a uniform greyish image background. The red circle highlights the focus position of the trapping laser. No immobilized particles are visible at the onset of the experiment (upper image), but an aggregate is clearly formed as time goes by. Fig. 2(c) shows examples of the temporal development of the SERS signal during this kind of experiment for the two test molecules. The SERS signal grows continuously, approaching a steady state, as more and more nanoparticles become trappe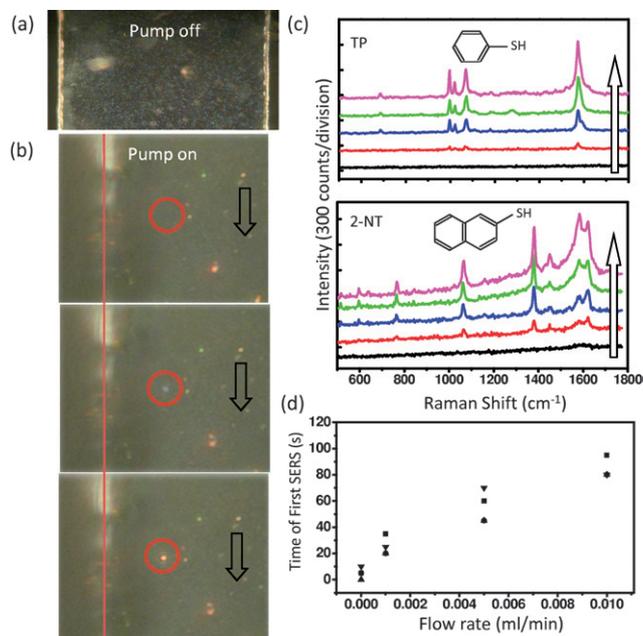d and subsequently aggregate on the surface. If the trapping laser is blocked, the SERS intensity gradually decreases, as particles begin to flow away from the aggregate (not shown). However, a small aggregate usually remains stuck on the substrate even in the absence of a trapping force. Examples of such residual aggregates are visible in Fig. 2(b). Their small size and miniscule area coverage imply that the same microfluidic channel can be used for a very large number of independent measurements, if the focus point is simply shifted laterally by a few microns in each SERS experiments. We should also note that the temporal development is a measure of the optical aggregation process rather than of molecular adsorption kinetics, since the Ag colloid and the TP/2-NT analyte mix already at the T-connector. This is illustrated in Fig. 2(d), which shows that the higher the flow rate, the longer it takes before the first SERS spectrum appears above the noise level. The reason is simply that the particles are less likely to become trapped if their velocity is high. This type of data could in principle be used to measure the depth of the optical potential well.

One of the advantages of the integrated system as a SERS sensor is the ease of switching between different analytes for multipurpose assays. To demonstrate this, we show in Fig. 3 an experiment in which small TP and 2-NT solution volumes, separated by air gaps, were introduced into one of the input tubes of the T-connector sequentially. When the pump is turned on, the Ag nanoparticles are thus incubated alternatively with TP and 2-NT beyond the T-connector. As shown in Fig. 3(b), alternate SERS spectra of TP and 2-NT were obtained from the optically aggregated Ag nanoparticles in the microfluidic channel. The small peaks at 1380 and 1625 cm^{-1} in the SERS spectra of TP are from residual 2-NT that has presumably physisorbed on the walls of the channel and then desorbed as the TP solution flows by.

SERS sensing through optical aggregation was also achieved in a Y-shaped microfluidic channel, see Fig. 4. The principal difference compared to the earlier scheme is that the colloid and analyte streams, which meet at the Y-conjunction, have much less time to mix. Incubation is further reduced through the laminar (parallel) flow
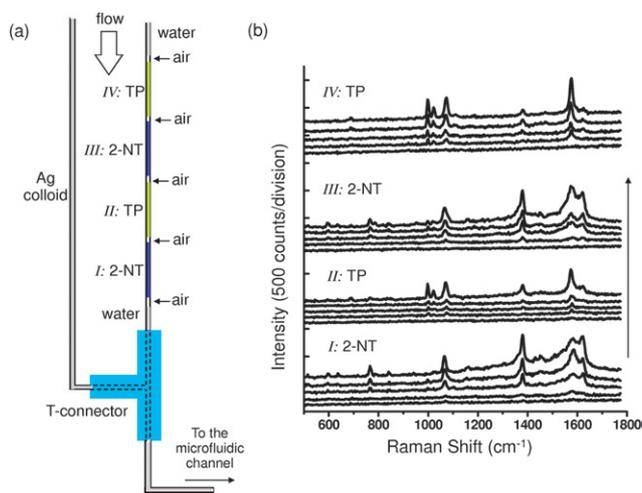

Fig. 2 Dark field (DF) images and time series SERS spectra during an optical trapping process in the microfluidic channel. (a) DF image of Ag nanoparticles with pump off (objective: 20×). (b) DF images of trapped Ag nanoparticles with a 100× objective (N.A. = 0.9) at a flow rate of 1.0 μl/min. (c) Time series SERS spectra of TP and 2-NT on trapped Ag nanoparticles with 1 s integration time and 10 s interval. (d) Time of the appearance of the first SERS spectra at different flow rates (four measurements at each flow rate).

Fig. 3 Consecutive detection of two different thiol molecules. (a) Scheme of the configuration. (b) Time series of SERS spectra from 2-NT and TP sequentially recorded as Ag nanoparticles, incubated with corresponding thiols, flow into the microfluidic channel and become optically aggregated. The flow rate was 1.0 μl/min and the integration time was 3 s.
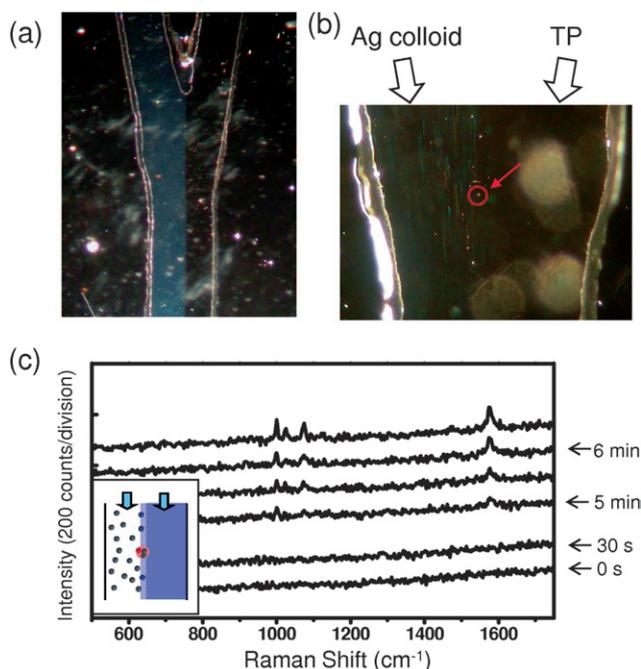
Fig. 4 SERS measurements using a Y-shaped channel. (a) DF image of the Y-shaped channel with Ag colloid (left) and TP solution (right). (b) DF image of trapped Ag nanoparticles at the interface. Flow rate: 1.0 μl/min. (c) SERS spectral series of TP measured from the trapped Ag nanoparticles in panel (b). The integration time was 3 s. Inset, scheme of the profile.

within the measurement channel, which only allows mixing through diffusion.[16,17] For SERS to be possible, optical aggregation therefore needs to be achieved close to the interface between the two streams. That this is possible is illustrated in Fig. 4(c), which shows a TP SERS spectral series obtained with the NIR laser focused directly at the interface. However, the time before the first SERS spectrum appears is much longer than that in the T-connector experiments, and the SERS intensity increases much slower with time. This is partly due to the reduced concentration of Ag colloid and TP at the interface, compared to that in the centre of the streams, but the main reason is probably the reduced incubation time. Although the spectral quality obtained in the Y-channel experiments is clearly inferior to what could be achieved in the T-connector scheme, the results points to the interesting possibility of quantifying molecular adsorption kinetics using SERS measurements. Similar to what has been recently reported in single cell studies, this should be possible if single nanoparticles or small clusters could be trapped in three dimensions (3D) and then quickly moved into the analyte stream for SERS readout.[18,19]

In summary, we successfully integrated SERS spectroscopy, laser tweezing and microfluidics. Ag colloid and analytes were injected separately and mixed in a T-connector or met at the conjunction of a Y-shaped channel. A focused NIR laser beam trapped and optically aggregated Ag nanoparticles from the flow at the bottom of the channel, thus forming an efficient SERS substrate, while a separate green laser beam was used for Raman excitation. Consecutive detection of two different analytes, TP and 2-NT, alternately filling the input tubing, was achieved. This demonstrates the ease of switching between different analytes for multipurpose assays. Although a number of improvements to the described schemes are possible, such as surface functionalization of the channels to decrease analyte adsorption, surface functionalization of Ag particles to facilitate non-thiol species adhesion, higher NIR power and/or better optics to enable 3D-trapping and obstacles in the channels to break the laminar flow and improve mixing, we consider the results promising for further development of lab-on-a-chip based SERS sensors.

Acknowledgements

Notes and references

1 M. Moskovits, *Rev. Mod. Phys.*, 1985, **57**, 783–828.
2 H. Xu, E. J. Bjerneld, M. Käll and L. Börjesson, *Phys. Rev. Lett.*, 1999, **83**, 4357–4360.
3 K. Faulds, R. E. Littleford, D. Graham, G. Dent and W. E. Smith, *Anal. Chem.*, 2004, **76**, 592–598.
4 K. E. Shafer-Peltier, C. L. Haynes, M. R. Glucksberg and R. P. Van Duyne, *J. Am. Chem. Soc.*, 2003, **125**, 588–593.
5 S. Lal, N. K. Grady, J. Kundu, C. S. Levin, J. B. Lassiter and N. J. Halas, *Chem. Soc. Rev.*, 2008, **37**, 898–911.
6 L. Gunnarsson, E. J. Bjerneld, H. Xu, S. Petronis, B. Kasemo and M. Käll, *Appl. Phys. Lett.*, 2001, **78**, 802–804.
7 L. A. Dick, A. D. McFarland, C. L. Haynes and R. P. Van Duyne, *J. Phys. Chem. B*, 2002, **106**, 853–860.
8 K. Faulds, D. Graham and W. E. Smith, *Anal. Chem.*, 2004, **76**, 412–417.
9 H. Wang, C. S. Levin and N. J. Halas, *J. Am. Chem. Soc.*, 2005, **127**, 14992–14993.
10 T. Park, S. Lee, G. H. Seong, J. Choo, E. K. Lee, Y. S. Kim, W. H. Ji, S. Y. Hwang, D. G. Gweon and S. Lee, *Lab Chip*, 2005, **5**, 437–442.
11 K. R. Strehle, D. Cialla, P. Rösch, T. Henkel, M. Köhler and J. Popp, *Anal. Chem.*, 2007, **79**, 1542–1547.
12 B. D. Piorek, S. J. Lee, J. G. Santiago, M. Moskovits, S. Banerjee and C. D. Meinhart, *PNAS*, 2007, **104**, 18898–18901.
13 F. Svedberg and M. Käll, *Faraday Discuss.*, 2006, **132**, 35–44.
14 F. Svedberg, Z. Li, H. Xu and M. Käll, *Nano Lett.*, 2006, **6**, 2639–2641.
15 P. C. Lee and D. Meisel, *J. Phys. Chem.*, 1982, **86**, 3391–3395.
16 J. Atencia and D. J. Beebe, *Nature*, 2005, **437**, 648–655.
17 T. M. Squires and S. R. Quake, *Rev. Mod. Phys.*, 2005, **77**, 977–1026.
18 E. Eriksson, J. Enger, B. Nordlander, N. Erjavec, K. Ramser, M. Goksör, S. Hohmann, T. Nyström and D. Hanstorp, *Lab Chip*, 2007, **7**, 71–76.
19 J. Prikulis, F. Svedberg, M. Käll, J. Enger, K. Ramser, M. Goksör and D. Hanstorp, *Nano Lett.*, 2004, **4**, 115–118.